$Arg^{615}Cys$ Substitution in Pig Skeletal Ryanodine Receptors Increases Activation of Single Channels by a Segment of the Skeletal DHPR II-III Loop

Esther M. Gallant, Suzanne Curtis, Suzy M. Pace, and Angela F. Dulhunty
Muscle Research Group, John Curtin School of Medical Research, P.O. Box 334, Canberra, ACT 2601, Australia

ABSTRACT The effect of peptides, corresponding to sequences in the skeletal muscle dihydropyridine receptor II-III loop, on Ca^{2+} release from sarcoplasmic reticulum (SR) and on ryanodine receptor (RyR) calcium release channels have been compared in preparations from normal and malignant hyperthermia (MH)-susceptible pigs. Peptide A (Thr^{671}-Leu^{690}; 36 μM) enhanced the rate of Ca^{2+} release from normal SR (SR_N) and from SR of MH-susceptible muscle (SR_{MH}) by 10 $\pm$ 3.2 nmole/mg/min and 76 $\pm$ 9.7 nmole/mg/min, respectively. Ca^{2+} release from SR_N or SR_{MH} was not increased by control peptide NB (Gly^{689}-Lys^{708}). AS (scrambled A sequence; 36 μM) did not alter Ca^{2+} release from SR_N, but increased release from SR_{MH} by 29 $\pm$ 4.9 nmoles/mg/min. RyR channels from MH-susceptible muscle (RyR_{MH}) were up to about fourfold more strongly activated by peptide A ($\geq$1 nM) than normal RyR channels (RyR_N) at $-$40 mV. Neither NB or AS activated RyR_N. RyR_{MH} showed an $\sim$1.8-fold increase in mean current with 30 μM AS. Inhibition at +40 mV was stronger in RyR_{MH} and seen with peptide A ($\geq$0.6 μM) and AS ($\geq$0.6 μM), but not NB. These results show that the $Arg^{615}Cys$ substitution in RyR_{MH} has multiple effects on RyRs. We speculate that enhanced DHPR activation of RyRs may contribute to increased Ca^{2+} release from SR in MH-susceptible muscle.

INTRODUCTION

Contraction of striated muscle depends on Ca^{2+} release from the terminal cisternae (TC) of sarcoplasmic reticulum (SR) through ryanodine receptor (RyR) calcium release channels. During excitation-contraction coupling (EC coupling) in skeletal muscle, an L-type Ca^{2+} channel (dihydropyridine receptor, DHPR) senses T-tubule depolarization and transmits an activating signal to the RyR. The signal is transmitted via a protein-protein interaction which requires the loop between the second and third repeats of the skeletal DHPR α_1 subunit (II-III loop, Tanabe et al., 1990). A region important for binding of the II-III loop is located on the skeletal RyR between Arg^{1076} and Asp^{1112} (Leong and Maclennan, 1998). Functional interactions between the skeletal DHPR II-III loop and skeletal RyRs have been described. For example, the II-III loop increases [^{3}H]ryanodine binding to SR vesicles, and activates purified RyR channels in lipid bilayers (Lu et al., 1994, 1995). A short peptide, corresponding to Thr^{671}-Leu^{690} of the skeletal DHPR II-III loop (peptide A), activates Ca^{2+} release from SR, (El-Hayek et al., 1995; El-Hayek and Ikemoto, 1998; Dulhunty et al., 1999). At $-$40 mV, peptide A ($\geq$10 nM) activates rabbit skeletal RyRs, but at +40 mV, peptide A ($\geq$1 μM) inhibits channels because the positively charged peptide blocks the channel pore (Dulhunty et al., 1999). A different II-III loop peptide, peptide C (724–760) inhibits activation of Ca^{2+} release from SR by peptide A (El-Hayek et al., 1995; El-Hayek and Ikemoto, 1998).

Because of the ability of the skeletal II-III loop and peptide A to activate RyRs, it has been suggested that binding of the A region of the DHPR to the RyR is a step in EC coupling (El-Hayek et al., 1995; El-Hayek and Ikemoto, 1998). Although the A region peptide is undeniably a high affinity activator of the RyR, its precise role in EC coupling remains to be determined. Skeletal EC coupling occurs when the A region contains either a skeletal, cardiac, or scrambled sequence; skeletal EC coupling cannot proceed unless the II-III loop contains a skeletal sequence between residues 725 and 742 (Nakai et al., 1998; Proenza et al., 2000), which is encompassed in peptide C. Curiously, the cardiac DHPR II-III loop also increases the activity of skeletal RyRs (Lu et al., 1994, 1995). Therefore, perhaps not surprisingly, binding of the II-III loop, or the 20-amino acid peptide A, has less rigid isoform specificity than the full EC coupling process. The experiments with dysgenic myocytes (Nakai et al., 1998; Proenza et al., 2000) do not give quantitative or kinetic information about EC coupling. It is possible that signal transmission during normal skeletal EC coupling occurs through both the A and C regions, but that some Ca^{2+} release from the SR can be induced via the C region alone. The functional properties of the A peptide continue to be investigated (i) because it is a high affinity specific activator of the RyR and thus useful for probing RyR function and (ii) because the A region may play a role in EC coupling.

The skeletal RyR is altered in a potentially lethal manner by approximately half of the mutations that lead to susceptibility to malignant hyperthermia (MH; Loke and Maclennan, 1998; Jurkat-Rott et al., 2000). In humans, 22 MH mutations have been identified at 20 different amino acid

Received for publication 3 May 2000 and in final form 17 January 2001.
Address reprint requests to Dr. A. F. Dulhunty, John Curtin School of Medical Research, Australian National University, PO Box 334, Canberra, ACT 2601, Australia. Tel.: 61-6-249-4491; Fax: 61-6-249-4761; E-mail: angela.dulhunty@anu.edu.au.

0006-3495/01/04/1769/14 $2.00

residues in the RyR and two MH mutations at one residue in the DHPR (Jurkat-Rott et al., 2000). A single amino acid substitution of Arg^{614} to Cys is responsible in 4% of MH-susceptible humans, and the same substitution at residue 615 of the RyR is found in all MH-susceptible pigs. Fifteen MH-linked RyR mutations are associated with an increased sensitivity to caffeine-induced Ca^{2+} release when recombinant DNA for the mutant RyRs was expressed in heterologous systems (Tong et al., 1997). Only two identified mutants have been studied in detail in muscle cells and/or muscle-derived preparations: arg^{615}cys in pigs and gly^{2434}arg in humans. A comparison of these mutants demonstrated remarkable similarities in RyR abnormalities, including enhanced sensitivity to both caffeine and calcium (Richter et al., 1997). Porcine MH SR vesicles are characterized by a greater than normal rate of Ca^{2+}-induced Ca^{2+} release (Kim et al., 1984); MH RyR channels have reduced inhibition by millimolar concentrations of Ca^{2+} (Fill et al., 1991; Shomer et al., 1993) or Mg^{2+} (Laver et al., 1997). Both of these abnormalities would presumably lead to enhanced Ca^{2+} release from SR during EC coupling (Ohta et al., 1989) and increased force production (Gallant et al., 1980) in MH muscles. Whether or not resting cytoplasmic $[Ca^{2+}]$ is increased in MH muscles remains controversial (Mickelson and Louis, 1996), and resting $[Ca^{2+}]$ is not elevated when RyRs with MH mutations are expressed in heterologous systems (Otsu et al., 1994; Tong et al., 1997, 1999). Such an elevation could indicate greater than normal Ca^{2+} leak from the SR of MH-susceptible muscles.

It has been suggested that reduced Mg^{2+} inhibition could be responsible for a higher resting cytoplasmic $[Ca^{2+}]$ and enhanced EC coupling in muscle from MH-susceptible pigs (Laver et al., 1997). It is thought that RyRs are chronically inhibited by Mg^{2+} under resting conditions, and EC coupling proceeds after a decrease in the affinity of RyRs for Mg^{2+} (Lamb and Stephenson, 1991). Although the reduced Mg^{2+} inhibition explains many of the effects of the Arg^{615}Cys substitution on EC coupling, other aspects of RyR_{MH} activity relevant to EC coupling have not been examined. Therefore, we have compared the effects of peptide A on the activity of normal RyRs and on RyRs from MH-susceptible pig muscle.

We find that peptide A activation of Ca^{2+} release from SR of MH-susceptible pigs is eightfold greater than that from SR of normal pigs. The enhancement of single RyR channel activity, at -40 mV, by peptide A is also two- to fourfold greater in RyR_{MH} as compared to RyR_N. This activation is specific for the native sequence of peptide A. Activation is not seen with peptide NB, corresponding to a sequence in a different region of the skeletal II-III loop, whereas lesser activation is seen with a scrambled sequence of the peptide (peptide AS). Inhibition of RyR channels at $+40$ mV by peptide A and peptide AS is also enhanced in RyR_{MH}. The results show that the point mutation in MH can have multiple effects on RyR activity. It is possible that stronger binding of the peptide A region of the DHPR to the RyR_{MH} may contribute to greater Ca^{2+} release from the SR during EC coupling in MH-susceptible muscle.

METHODS

Materials

Chemicals and biochemicals were from Sigma-Aldrich (Castle Hill, Australia). DHPR II-III loop peptide synthesis has been described previously (Dulhunty et al., 1999). Peptides were synthesized with purification to 98 to 100% using HPLC, mass spectroscopy, and NMR. Stock peptide solutions (~2 mM) were prepared in H_2O and frozen in aliquots of 20 μl. Precise stock solution concentrations were determined by Auspep Proprietry Ltd. (Melbourne, Australia). Peptides used in this study were:

Peptide A:

^{671}Thr Ser Ala Gln Lys Ala Lys Ala Glu Glu Arg Lys Arg Arg Lys Met Ser Arg Gly Leu^{690}

Peptide NB:

^{689}Gly Leu Pro Asp Lys Thr Glu Glu Glu Lys Ser Val Met Ala Lys Lys Leu Glu Gln Lys^{708}

Peptide AS:

Thr Arg Lys Ser Arg Leu Ala Arg Gly Gln Lys Ala Lys Ala Lys Ser Glu Met Arg Glu

Biological material and caffeine-halothane contracture test for MH susceptibility

The methods for genetic testing, anaesthetic techniques, muscle dissection, caffeine-halothane contracture testing, preparation of SR vesicles, and single channel recording have been described previously (Otsu et al., 1992; Owen et al., 1997; Laver et al., 1997). Muscle and blood samples were obtained from 3 homozygous normal pigs (1 Belgium Landrace and 2 Landrace) and 3 homozygous MH pigs (2 Belgium Landrace and 1 Landrace) aged ~4 months. Each animal was genetically tested for normal or MH RyR allele containing either Arg^{615} or Cys^{615}. The SR preparations were from the same animals as those used in Laver et al. (1997) and Haarmann et al. (1999). All fiber bundles from the 3 homozygous normal animals failed to respond to halothane or 2 mM caffeine, whereas all fiber bundles from the 3 homozygous MH animals developed tension in response to both drugs.

Isolation of SR vesicles

The preparation of crude SR vesicles was based on Meissner (1984) and Ma et al. (1995). Freshly dissected back and leg muscle was washed in cold phosphate-buffered saline containing 2 mM EGTA (pH 7.0), trimmed of fat and connective tissue, cut into cubes, and either frozen in liquid N_2 and stored at -70°C or freshly processed. The fresh or thawed muscle cubes were suspended in 5 mM Tris maleate, 100 mM NaCl, 2 mM EDTA, and 0.1 mM EGTA, pH 6.8 (5 ml/g of tissue). The muscle was homogenized in a Waring Blendor with four 15-s high-speed bursts. The homogenate was centrifuged at $2600 \times g$ for 30 min and the supernatant filtered through cotton gauze and centrifuged at $10,000 \times g$ for 30 min. The pellet (P2) was collected and the supernatant was centrifuged again at $35,000 \times g$ and the

pellet (P3) collected. Pellets P2 and P3 were resuspended in 5 mM Tris-2-(*N*-morpholino)ethanesulphonic acid (Tris-MES), 300 mM sucrose, 100 mM KCl, and 2 mM dithiothreitol, pH 6.8. Aliquots of the suspensions were frozen in liquid nitrogen and stored at −70°C. All buffers contained the protease inhibitors phenylmethylsulfonyl fluoride (0.7 mM), leupeptin (1 μg/ml), pepstatin A (1 μM), and benzamidine (1 mM).

Calcium release from SR vesicles

Extravesicular Ca^{2+} was monitored at 710 nm with the Ca^{2+} indicator, antipyrylazo III, using a Cary 3 Spectrophotometer (Varian, Sydney, Australia). Identical experiments at 790 nm showed that there were no changes in OD which would alter the rate of Ca^{2+} uptake measured at 710 nm. A step increase in OD upon addition of ruthenium red or caffeine, seen at both 710 nm and 790 nm, was subtracted from the data in Figs. 1 and 2 (Results). The temperature of the cuvette solution was thermostatically controlled at 25°C, and the solution was stirred with a magnetic stirrer. Ca^{2+} release was measured as described by Timerman et al. (1993). TC vesicles (100 μg of protein) were added to the cuvette, to a final volume of 2 ml of a solution containing 100 mM KH_2PO_4 (pH 7); 4 mM $MgCl_2$, 1 mM Na_2ATP, and 0.5 mM antipyrylazo III. Vesicles were partially loaded with Ca^{2+} by four sequential additions of $CaCl_2$, each initially increasing the extravesicular [Ca^{2+}] by ~7.5 μM (~15 nmoles). It was necessary to suppress Ca^{2+}, Mg^{2+}-ATPase activity after loading (using 200 nM thapsigargin; Sagara and Inesi, 1991), to allow extravesicular [Ca^{2+}] to increase after activation of the RyR. Peptide was then added, followed either by 10 mM caffeine (to determine RyR-releasable Ca^{2+} remaining in the SR vesicles) or by the RyR blocker ruthenium red (to a final concentration of 5 μM), to determine whether Ca^{2+} release from SR was via RyR channels. The Ca^{2+} ionophore A23187 (3 μg/ml) was finally added to release the Ca^{2+} remaining in the SR vesicles. A calibration curve for OD changes for a given increase in [Ca^{2+}] was established at the start of each experiment, using 4 sequential additions of 12.5 μM (25 nmoles) of $CaCl_2$.

Addition of H_2O alone to the cuvette after thapsigargin, produced a small decline in the rate of release of Ca^{2+}. This was measured for each experiment and the rate of Ca^{2+} release in the presence of peptide was appropriately corrected. The increase in OD for a given increase in extravesicular [Ca^{2+}] was ~40% less in the presence of 10 mM caffeine (see legend to Fig. 1). This factor was taken into account in calculations of releasable Ca^{2+}.

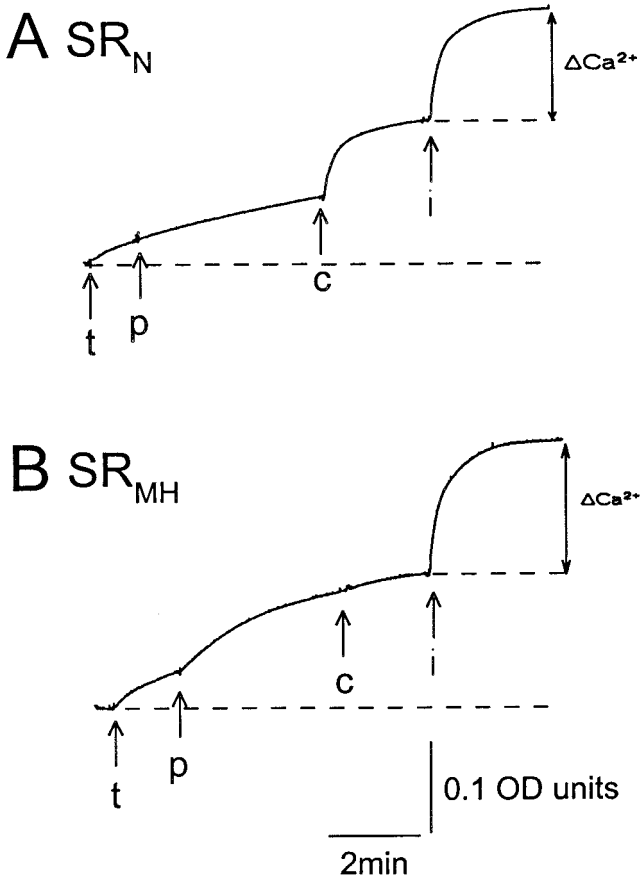

FIGURE 1 Increase in rate of Ca^{2+} release after addition of peptide A is greater in SR_{MH} than in SR_N. (*A*) and (*B*) show records of OD changes at 710 nm, with changes in extravesicular [Ca^{2+}], measured using antipyrylazo III as the Ca^{2+} indicator. SR vesicles were loaded with Ca^{2+} by an initial uptake of ~16 nmoles of Ca^{2+} plus four additions of 15 nmoles of Ca^{2+} (not shown). The first arrow (t) indicates addition of 200 nM thapsigargin to block the SR Ca^{2+} ATPase. The second arrow (p) indicates addition of 36 μM peptide A. Caffeine (10 mM) was added at the third arrow (c) before the ionophore A23187 (last arrow (i), 3 μg/ml). The vertical calibration is in OD units: an increase of 0.1 OD unit occurred with an increase in extravesicular Ca^{2+} of 18 nmoles before adding caffeine, or 31 nmoles after adding caffeine (see Methods). ΔCa^{2+} is the non-RyR releasable Ca^{2+} remaining in the SR after exposure to caffeine.

Lipid bilayer techniques

The lipid bilayer and single channel recording technique are described in Laver et al. (1997) and Dulhunty et al. (1999). Bilayers were formed from phosphatidylethanolamine, phosphatidylserine, and phosphatidylcholine (5:3:2 w:w) (Avanti Polar Lipids, Alabaster, AL) across an aperture with a diameter of 200 to 250 μm in the wall of a 1.0 ml Delrin cup (Cadillac Plastics, Australia). TC vesicles (final concentration, 10 μg/ml) were added to the *cis* chamber and stirred until vesicle incorporation was observed. The cytoplasmic side of channels incorporated into the bilayer faced the *cis* solution. The bilayer potential was controlled, and single channel activity was recorded using an Axopatch 200A amplifier (Axon Instruments, Foster City, CA). For experimental purposes, the *cis* chamber was held at ground and the voltage of the *trans* chamber controlled. Bilayer potential is expressed in the conventional way as $V_{cis} - V_{trans}$, (i.e., $V_{cytoplasm} - V_{lumen}$).

Bilayers were formed and vesicles incorporated into the bilayer using *cis* solutions containing 230 mM Cs methanesulphonate (CsMS), 20 mM CsCl, 1.0 mM $CaCl_2$, and 10 mM N-tris[hyroxymethyl]methyl-2-aminoethanesulfonic acid (TES), pH 7.4, adjusted with CsOH. The *trans* solution had the same composition, except that CsMS was 30 mM. The *cis* solution sometimes contained 500 mM mannitol to aid SR vesicle fusion and RyR incorporation into the bilayer. After incorporation, the *cis* solution was replaced (by perfusion) with an identical solution, except that [Ca^{2+}] was varied between 0.3, 10, and 100 μM, and buffered at 0.3 and 10 μM by 2 mM BAPTA, and 200 mM CsMS was added to the *trans* chamber to establish symmetrical conditions.

Recording and analysis of single channel activity

Currents were filtered at 1 kHz (10-pole low pass Bessel, −3dB) and digitized at 5 kHz. Analysis of single channel records (using Channel 2, developed by P. W. Gage and M. Smith, John Curtin School of Medical Research) yielded channel open probability (P_o), frequency of events (F_o), open times, closed times, and mean open (T_o) and closed (T_c) times, as well as mean current (I′). P_o, T_o, and T_c were measured by determining the number and duration of events in which the current exceeded a threshold level. An event discriminator set above the baseline noise at ~20% of the

maximum current, rather than the usual 50%, was used so that openings to both subconductance and maximum conductance levels were included in the analysis. In contrast, I′, the mean current, is the average of all data points in a record, in which the baseline is set to 0 pA. Ideally, in a channel lacking submaximal conductance activity, I′ approaches the single channel conductance as P_o approaches 1.0. The threshold detection method is very accurate in measuring openings when the peak amplitude of openings exceeds the event discriminator. However, the technique fails when the channel openings are to low conductance levels that are close to the baseline noise. In this case, mean current provides the most accurate method of measuring channel activity.

Bilayers that appeared to contain one channel under control conditions often showed multiple channel openings (i.e., a maximum conductance of 2 or 3 times the single channel conductance) after addition of peptide A. I′ provided an accurate measure of the current flowing through two or three channels after addition of peptide. The discriminator method was not used to measure activity when more than one channel was present in the bilayer because of the difficulty in deconvolution to meaningful single channel parameters. Since bilayers containing more than one channel could not be used for measurements of single channel parameters (i.e., P_o, T_o, and T_c) and since most bilayers eventually contained more than one channel, routine measurements of channel activity were done using mean current (I′) analysis. P_o was measured in the few records containing only one channel to assess how single channel activity was affected by the peptide.

Statistics

Average data is given as mean ± SEM. The significance of the difference between control and test values was tested a using either Student's *t*-test, either 1- or 2-sided and either for independent or paired data, as appropriate, or the nonparametric sign test (Minium et al., 1993). Differences were considered to be significant when $P \leq 0.05$.

RESULTS

Calcium release from sarcoplasmic reticulum vesicles

Ca^{2+} release from skeletal SR of normal (SR_N) and MH-susceptible (SR_{MH}) pig muscle was examined in vesicles that were loaded with Ca^{2+} followed by block of the Ca^{2+}, Mg^{2+}-ATPase with 200 nM thapisgargin. A time-dependent increase in extravesicular [Ca^{2+}] occurred after thapsigargin addition. The rate of calcium release increased further after adding peptide A (Fig. 1).

In the examples in Fig. 1, the rate of Ca^{2+} release from SR_N with thapsigargin was ~47 nmoles/mg/min and this increased to ~60 nmoles/mg/min after adding 36 μM peptide, showing a peptide-induced enhancement of 13 nmoles/mg/min (Fig. 1 *A*). Peptide A evoked stronger release from SR_{MH}; the rate increased from 66 nmoles/mg/min with thapsigargin to ~162 nmoles/mg/min after adding 36 μM peptide, with a peptide-induced enhancement of 96 nmoles/mg/min (Fig. 1 *B*).

The fraction of Ca^{2+} accumulated by SR_N and SR_{MH} that was not available for release through RyRs (presumably that not contained in terminal cisternae) was determined by exposing vesicles to 10 mM caffeine (~4 min after peptide addition), to release Ca^{2+} in TC vesicles through RyR channels, and then to the Ca^{2+} ionophore A23187 (3 μg/ml) to release all remaining Ca^{2+} (Fig. 1, *A* and *B*). The fraction of non-releasable Ca^{2+} was the difference between the Ca^{2+} released by caffeine and that released by the ionophore (ΔCa, Fig. 1; ΔCa is larger in SR_{MH} than in SR_N). Ruthenium red (10 μM) stopped Ca^{2+} release if it was added while extravesicular [Ca^{2+}] was increasing ($n = 8$, data not shown), showing that Ca^{2+} release after addition of thapsigargin, and release activated by peptide A, was through RyR channels.

On average the rate of Ca^{2+} release from SR_{MH} with thapsigargin of 53 ± 5.2 nM/mg/min ($n = 12$) was significantly greater than the 41 ± 2.2 nM/mg/min ($n = 13$) for SR_N. The rate of Ca^{2+} release induced by peptide A is the rate after peptide addition, minus the rate with thapsigargin (inset, Fig. 2). A release rate of 76 ± 9.7 nmole/mg/min ($n = 3$) from SR_{MH} induced by 36 μM peptide A was significantly greater than the rate of 10 ± 3.2 nmole/mg/min from SR_N ($n = 3$, Fig. 2). Comparable results were obtained from three SR_N and three SR_{MH} preparations.

Average nonreleasable Ca^{2+} was 16.5 ± 0.57 nmoles in SR_N and 20.3 ± 0.55 nmoles in SR_{MH}. Since ~60 nmoles of Ca^{2+} were loaded, non-RyR releasable Ca^{2+} fraction was 0.28 ± 0.01 in RyR_N and 0.34 ± 0.01 in RyR_{MH}. The significantly smaller nonreleasable Ca^{2+} in SR_N suggests that SR_N was more enriched in terminal cisternae than the SR_{MH}. The different fraction of nonreleasable Ca^{2+} indicated that the difference between peptide A-induced release from terminal cisternae was about eightfold greater in SR_{MH} than in SR_N (rather than the ~7.6-fold indicated by the uncorrected rates).

Control peptides NB and AS did not mimic the effects of peptide A. The rates of Ca^{2+} release from SR_N and SR_{MH}

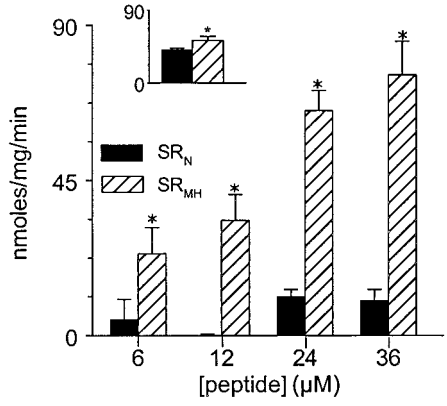

FIGURE 2 The initial rate of peptide A-enhanced Ca^{2+} release (nmoles/mg of TC vesicles/min) from SR_N is less than from SR_{MH}. The rate is the initial rate of release with peptide, minus the preceding rate with thapsigargin ($n = 3$ at each peptide concentration for each of SR_N and SR_{MH}). Filled bins show data from SR_N and cross-hatched bins show data for SR_{MH}. Data are averages ± SEM for TC vesicles from three different SR preparations. Asterisks show significant differences between data for SR_N and SR_{MH}. The insert shows average rates of Ca^{2+} release from SR_N and SR_{MH} in the presence of thapsigargin, just before addition of peptide ($n = 12$).

immediately after adding 36 μM NB (minus the rate with thapsigargin) were 8.2 $\pm$ 2.6 nmoles/mg/min (n = 4) and -1.1 ± 3.4 nmoles/mg/min (n = 4), respectively. Addition of AS resulted in excess release at rates of 6.3 $\pm$ 4.2 nmoles/mg/min (n = 4) and 29 $\pm$ 4.9 nmoles/mg/min (n = 4) for SR_N and SR_{MH}, respectively. The increase in Ca^{2+} release from SR_{MH} with AS was significant, but remained significantly less than that induced by peptide A.

RyR channel activity

Peptide A (0.6 nM to 30 μM) was added to the *cis* side of the bilayer, with 250/250 mM Cs^+ (*cis/trans*), at [Ca^{2+}]s of 3×10^{-7} M, 10^{-5} M, or 10^{-4} M (*cis*) and 10^{-3} M (*trans*). Initial experiments with 2 mM Na_2ATP in the *cis* solution failed to show convincing peptide A-induced activation of normal pig skeletal RyRs (RyR_N, n = 23) or RyRs from MH-susceptible pigs (RyR_{MH}, n = 25), although the usual peptide A-induced inhibition (Fig. 6 below) was seen in the presence *cis* Ca^{2+} = 100 μM. Thus experiments examining activation by peptide A were performed in the absence of ATP. Low levels of activity were recorded under these conditions. Table 1 shows that average mean current in bilayers containing 1 to 3 RyR_N or RyR_{MH} channels was between 0.2 and 2.5 pA before addition of peptide. This was 0.01 to 0.05 of the maximum current (+15 pA or −15 pA at +40 mV or −40 mV, respectively). There were no significant differences in control mean current between RyR_N and RyR_{MH}.

Activating effects of peptide A on channels at −40 mV

The strongest activating effects of peptide A in rabbit are seen at negative potentials where there is less peptide-induced inhibition (Dulhunty et al., 1999). Peptide A (*cis*, 0.6 μM and 30 μM) activated RyR_N and RyR_{MH} channels at −40 mV (Fig. 3). The increase in activity was not associated with an increase in the single channel conductance. The conductance of the RyR_N channel was in fact reduced with 30 μM peptide, due to the peptide's inhibitory

TABLE 1 Average mean current under control conditions (I′c) in pA for RyR_N and RyR_{MH} with 300 nM, 10 μM, and 100 μM *cis* Ca^{2+}

	RyR_N			RyR_{MH}		
Cis[Ca^{2+}]	n	−40mV I′c (pA)	+40mV I′c (pA)	n	−40mV I′c (pA)	+40mV I′c (pA)
300 nM	8	0.68 ± 0.21	0.67 ± 0.24	9	0.94 ± 0.29	0.94 ± 0.50
10 μM	8	1.16 ± 0.17	1.22 ± 0.30	10	1.77 ± 0.85	1.24 ± 0.44
100 μM	6	**1.76 ± 0.4**	**1.62 ± 0.41**	6	1.33 ± 0.26	2.48 ± 0.98

Data are given as mean ± SEM. The number of experiments is listed under n. The data in **bold print** are significantly different (Student's t-test from data obtained with 300 nM *cis* Ca^{2+}.

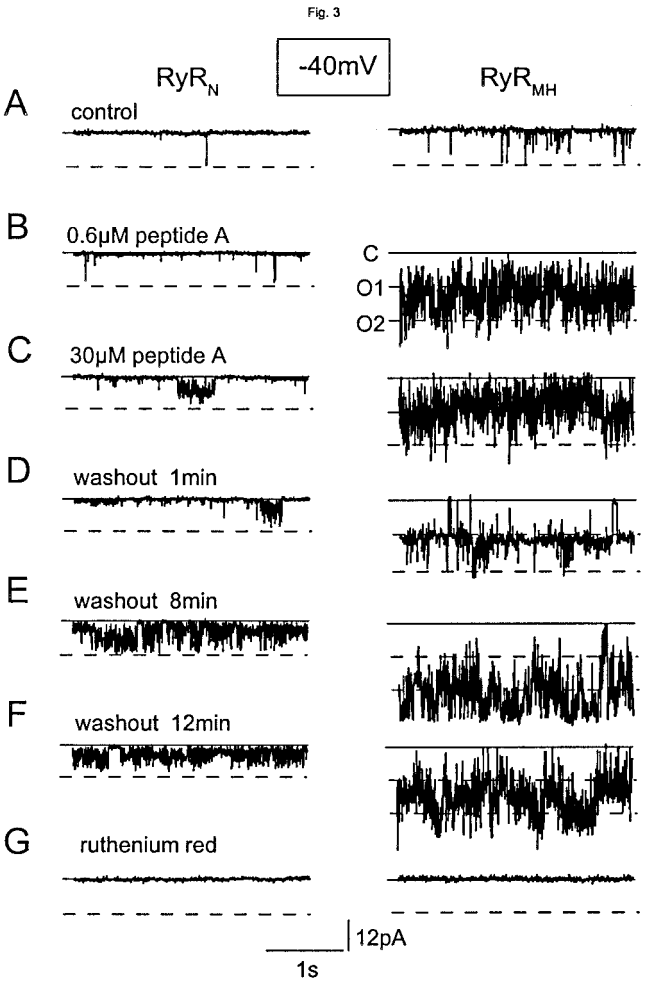

FIGURE 3 Single channel activity at −40 mV is enhanced after adding 0.6 μM or 30 μM peptide A and activation is greater in RyR_{MH} (right panel) than RyR_N (left panel). Records were obtained with 10 μM *cis* Ca^{2+}. (*A*) Control; (*B*) after adding 0.6 μM peptide A to the *cis* chamber; (*C*) after increasing *cis* (peptide A concentration) to 30 μM; (*D–F*), 1, 8, and 12 min, respectively, after perfusion of the *cis* chamber with peptide-free solution; (*G*) 1 min after adding 30 μM *cis* ruthenium red. The solid line shows the zero current (closed, C); the broken line shows the maximum open channel conductance for one channel (O1), or two channels (O2) in RyR_{MH}.

action. One RyR_{MH} channel is apparent in Fig. 3 under control conditions and a second and third channel are seen with peptide A. Washout of peptide with 10 volumes of *cis* solution caused an increase in activity (discussed below). Activity of RyR_N and RyR_{MH} was abolished by 30 μM *cis* ruthenium red added at the end of the experiment (Fig. 3 *G*).

A history plot of mean current during similar experiments with 10 or 100 μM *cis* Ca^{2+} are shown in Fig. 4. I′ progressively increased during exposure to increasing concentrations of peptide and there was a further increase after washing out 30 μM peptide. A greater increase in activity with peptide addition is seen in RyR_{MH} than in RyR_N. The average normalized mean current (I′p/I′c) also increased

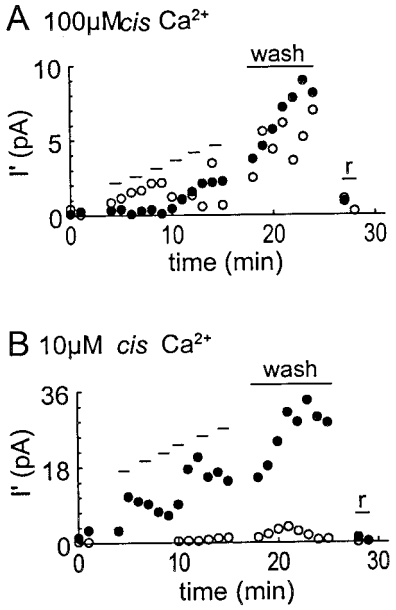

FIGURE 4 Continuous time course of channel activity during exposure to peptide A, washout of peptide A and exposure to ruthenium red. The mean current (I′) in 30-s recordings at −40 mV (each separated by a 30-s recording at +40 mV). *A* and IB, with 100 μM *cis* Ca^{2+}; data from one bilayer with 2 RyR_N (*open circles*) and a second bilayer with 2 RyR_{MH} channels (*filled circles*). *C* and *D*, with 10 μM *cis* Ca^{2+}; data from one bilayer with 2 low activity RyR_N channels (*open circles*) and from a second bilayer with 3 relatively high activity RyR_{MH} (*filled circles*), to compare analysis techniques. Each data point is from a 30-s recording at −40 mV. Successive points are separated by 30 s at +40 mV (not shown). The initial two points in each graph show control activity. Peptide A was then added to progressively increase concentration from 0.6 nM to 6 nM, 60 nM, 600 nM, 6 μM, and 306 μM (indicated by short horizontal lines), with 120 s at each peptide concentration. Peptide was then perfused out of the *cis* chamber and washout effects recorded during the period labeled "wash". Finally, ruthenium red was added (horizontal line labeled *r*).

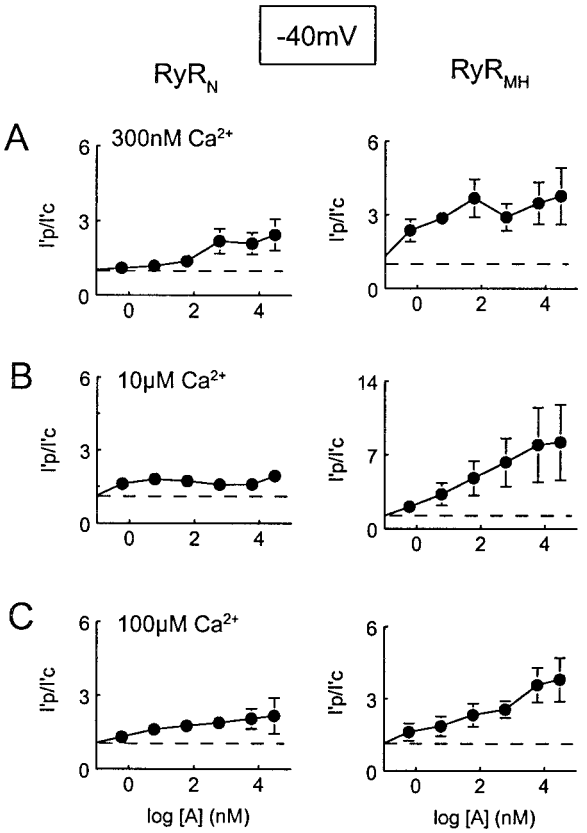

FIGURE 5 Peptide A causes a greater increase in mean current at −40 mV in RyR_{MH} (*right*) than in RyR_N (*left*). Relative mean current (I′p/I′c, where I′p is I' in the presence of peptide and I′c is I' under control conditions) is plotted against the logarithm of peptide A concentration in nM. Symbols show average I′p/I′c and vertical bars show ±1 SEM where this is greater than the dimensions of the symbol. Results were obtained with: (*A*) 300 nM *cis* Ca^{2+} (n = 11 for RyR_N; n = 8 for RyR_{MH}); (*B*) 10 μM *cis* Ca^{2+} (n = 19 for RyR_N; n = 15 for RyR_{MH}); (*C*) 100 μM *cis* Ca^{2+} (n = 9 for RyR_N; n = 10 for RyR_{MH}).). On average, peptide A caused up to a twofold increase in I′p/I′c for RyR_N at each *cis* $[Ca^{2+}]$. RyR_{MH} showed greater increases in the normalized mean current at −40 mV with peptide A at each *cis* $[Ca^{2+}]$, with 4.0- to 7.5-fold increases in I′p/I′c.

more in RyR_{MH} than in RyR_N with peptide A at each *cis* $[Ca^{2+}]$ (Fig. 5, *A–C*). Maximum activation of both RyR_N and RyR_{MH} at was achieved with 0.6 to 6 μM peptide A.

Single channel parameters were measured from records with only one channel active in the bilayer before and during exposure to the peptide (Fig. 6). Such experiments were rare because summed openings of multiple (two or three) channels usually became obvious after addition of activating concentrations of peptide. Therefore, the numbers of channels analyzed in this way were too few to establish the Ca^{2+} dependence of single channel parameters or the effects of Ca^{2+} on peptide-induced changes in the parameters. The effects of cytoplasmic Ca^{2+} concentration on peptide A-induced activation are best seen in Fig. 5.

In the set of experiments used for single channel analysis, activity tended to be low ($P_o < 0.1$) under all control conditions. Peptide A caused an increase in P_o, T_o, and F_o and a decrease in T_c in all 7 RyR_N channels and in 8 of 9 RyR_{MH} channels at −40 mV (Fig. 6, *A–D*). There was no consistent difference between parameter values for RyR_N and RyR_{MH} under control conditions at ≤100 μM *cis* Ca^{2+} (see also Fill et al., 1990; Shomer et al., 1993; Laver et al., 1997). However, in the presence of the peptide at −40 mV, P_o, and T_o tended to be greater in RyR_{MH} than in RyR_N (Fig. 6, *A* and *B*).

Overall, the results suggest that peptide A had similar actions on the gating of RyR_N and RyR_{MH} channels, reducing the mean closed time and increasing the duration and frequency of channel openings. The effect of the $Arg^{615}Cys$ substitution in RyR_{MH} was to amplify these actions of the peptide, particularly the increase in the duration of channel opening.

Activating and inhibiting effects of peptide A on RyR channels at +40 mV

At +40 mV, RyR_N and RyR_{MH} channels were activated by peptide A at 0.6 μM, but inhibited by peptide at 30 μM

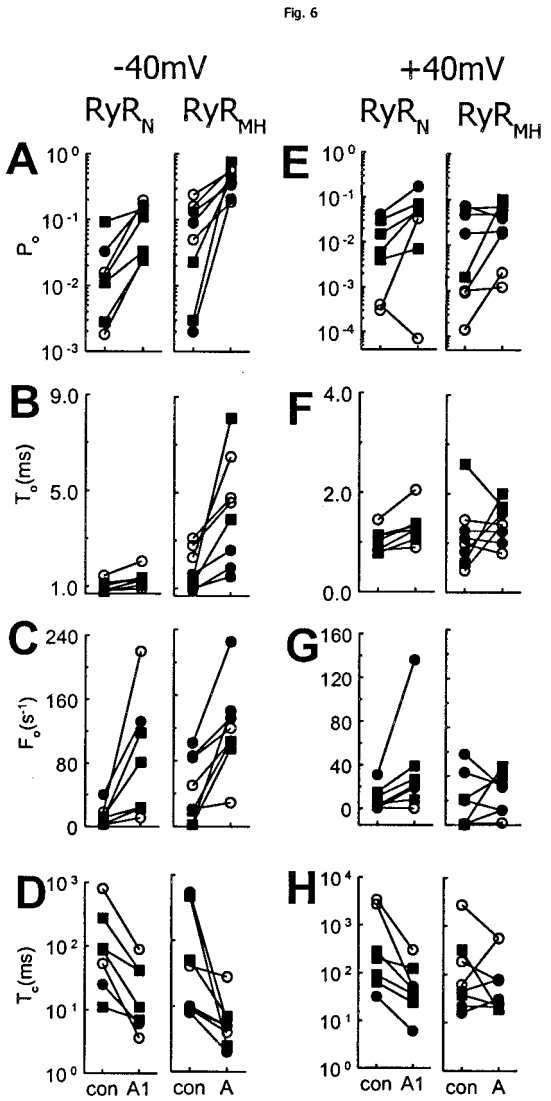

FIGURE 6 The effects of peptide A on single channel characteristics of RyR_N and RyR_{MH}. Analysis was performed on 120 s of channel activity before addition of peptide and 120 s of activity at the peptide concentration giving greatest activation, i.e., between 0.6 and 30 μM. Channel activity was measured at −40 mV (*A–D*) and at +40 mV (*E–H*). Data is shown for open probability (P_o, *A* and *E*), mean open time (T_o, *B* and *F*), opening frequency (F_o, *C* and *G*) and mean closed time (T_c, *D* and *H*). The symbols show data for individual channels with *cis* Ca^{2+} concentrations of 300 nM (○), 10 μM (■), and 100 μM (●). Solid lines connect data for control conditions (con) with data obtained in the presence of peptide A (A).

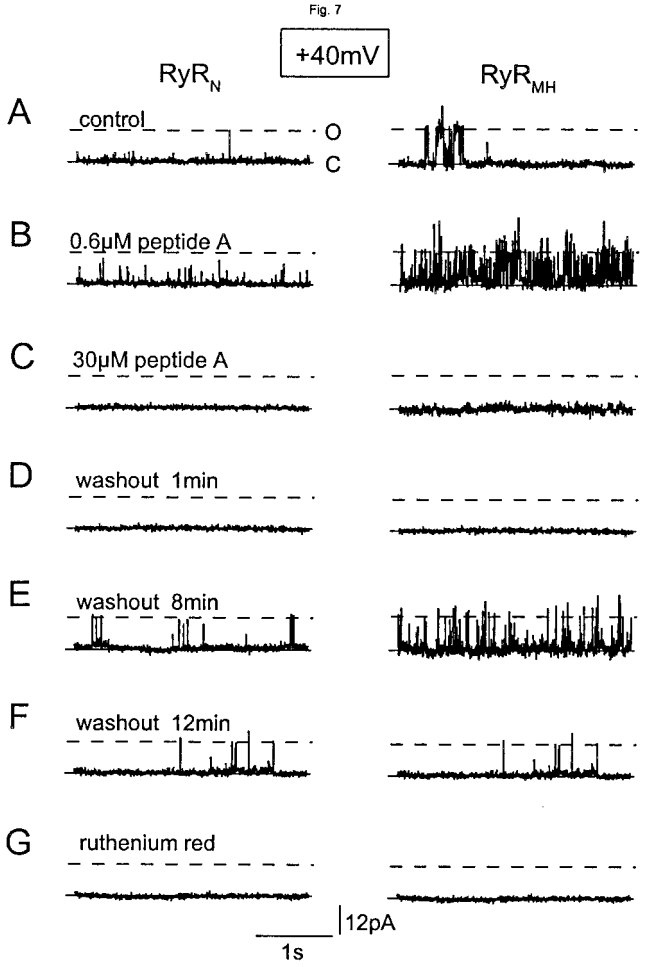

FIGURE 7 Single channel activity at +40 mV is enhanced after adding 0.6 μM peptide A, but is inhibited with 30 μM peptide A. Activation is greater in RyR_{MH} (right panel) than RyR_N (left panel). Records are from the same channels shown in Fig. 3 with 10 μM *cis* Ca^{2+}. (*A*) control; (*B*) after adding 0.6 μM *cis* peptide A; (*C*) after increasing *cis* [peptide A] to 36 μM; (*D–F*), 1, 8, and 12 min, respectively, after perfusion of the *cis* chamber with peptide-free solution; (*G*) 1 min after adding 30 μM ruthenium red to the *cis* chamber. The solid line shows the zero current (closed, C); the broken line shows the maximum open single channel conductance (O).

(Fig. 7, *A–C*). Inhibition resulted in channel openings to lower conductance levels, which are apparent in RyR_N with 0.6 μM peptide (Fig. 7 *B*). Activation by 0.6 μM peptide at +40 mV was greatest in the RyR_{MH} channel. Perfusion of peptide A out of the *cis* chamber at +40 mV was followed by a slow increase, and then a decline in channel opening (Fig. 7, *D–F*). The increase in activity after perfusion was associated with recovery of the maximum open conductance, confirming that the reduced conductance with 0.6 μM peptide was due to the inhibitory effect of the peptide.

Normalized mean current at +40 mV increased with peptide A between 0.6nM and 0.6 μM and then, in contrast to effects at −40 mV, declined with inhibition at higher [peptide] under most conditions (Fig. 8). Both the increase in average I′p/I′c and the subsequent decline with increasing [peptide] at +40 mV were more pronounced in RyR_{MH} than in RyR_N. As in rabbit (Dulhunty et al., 1999) the strongest inhibition by peptide A was seen in both RyR_N and RyR_{MH} when *cis* Ca^{2+} was 100 μM.

The peptide-induced changes in single channel parameters were smaller and less consistent at +40 mV than at −40 mV (Fig. 6, *E–H*). For example, an increase in T_o was seen in 5 of 7 RyR_N channels and 3 of 9 RyR_{MH} channels.

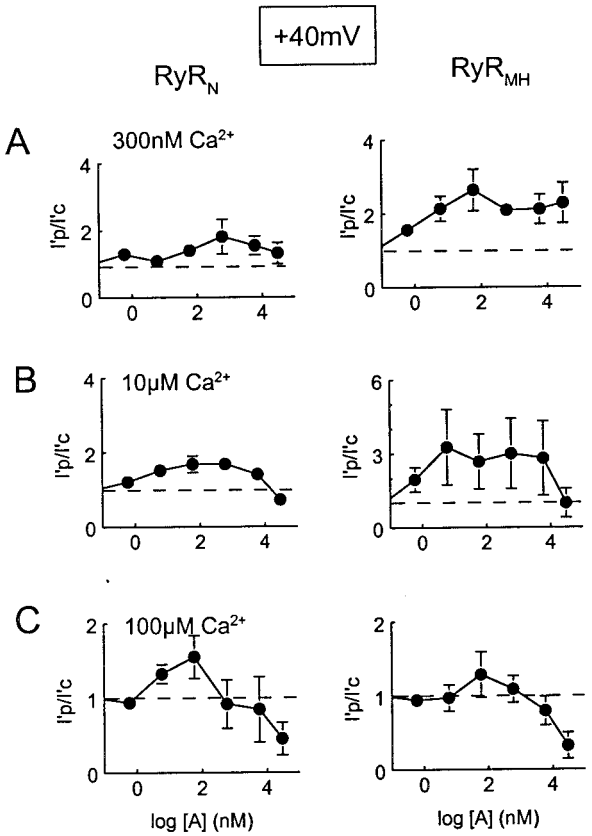

FIGURE 8 Peptide A causes a greater decrease in average mean current at +40 mV in RyR_{MH} (right column) than in RyR_N (left column). Relative mean current is plotted as described for Fig. 5. Symbols show average I′p/I′c and vertical bars show ±1 SEM where this is greater than the dimensions of the symbol. Results were obtained with: (*A*) 300 nM *cis* Ca^{2+} ($n = 11$ for RyR_N; $n = 8$ for RyR_{MH}); (*B*) 10 μM *cis* Ca^{2+} ($n = 19$ for RyR_N; $n = 15$ for RyR_{MH}); (*C*) 100 μM *cis* Ca^{2+} ($n = 9$ for RyR_N; $n = 10$ for RyR_{MH}). There were 3.4-fold and 5.0-fold declines in average I′p/I′c, from the maximum peptide-activated levels, in RyR_{MH} with 30 μM peptide and 10 μM or 100 μM *cis* Ca^{2+} respectively, compared with 2.1-fold and 1.6-fold falls in I′p/I′c for RyR_N. I′p/I′c did not fall significantly in RyR_N with 300 nM Ca^{2+}.

This was presumably due to the competing activating and inhibiting effects of the peptide at +40 mV, since inhibition decreases T_o (Dulhunty et al., 1999).

Peptide A washout

The increases in channel activity after washout of peptide (Figs. 3, 4, and 7) were also seen in rabbit RyRs and were thought to reflect exposure of a high-affinity activating effect after washout of a lower affinity peptide A-induced inhibition (Dulhunty et al., 1999). The slower removal of peptide from its activating site after washout is consistent with a higher affinity binding to the activation site in RyR_N and RyR_{MH}, whereas faster removal from the inhibition site is consistent with lower affinity binding to the inhibition site in RyR_N and RyR_{MH}. The washout activation suggests that channel activity in the presence of the peptide is a sum of simultaneous activation and inhibition. The time to peak activity after washout reflects the time course of removal of inhibition. The lack of full reversal of activation after 7 to 12 min suggests that the peptide remained bound to its activation site for this time, as might be expected with high affinity binding. The slower washout of activation in RyR_{MH} suggests stronger binding of peptide A to the activation site on RyR_{MH}.

The increase in RyR activity after removal of peptide A may provide a more accurate indication of the ability of the peptide to activate RyR_N and RyR_{MH} than channel activity in the presence of the peptide, which is the sum of activation and inhibition. Long-term washout experiments were performed with 10 μM and 100 μM *cis* Ca^{2+}. I′p/I′c increased significantly after washout and was significantly greater at −40 mV than at +40 mV under all conditions (Fig. 9). I′p/I′c after washout at −40 mV was significantly greater in RyR_{MH} than in RyR_N with both 10 μM and 100 μM *cis* Ca^{2+} (note the different scales on the *y* axes). Curiously, there was no difference between RyR_N and RyR_{MH} in

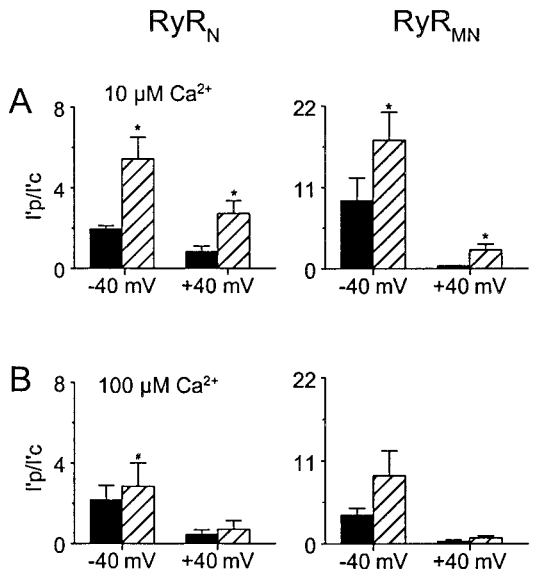

FIGURE 9 Mean current increases after peptide A removal from the *cis* chamber. The increase is significantly greater at −40 mV in RyR_{MH} (right panel) than in RyR_N (left panel) at each *cis* [Ca^{2+}] (note the different scales on the *y* axes; see text). The results are from a subset of data in which RyR_N or RyR_{MH} channels were held for 6 to 10 min after washout of peptide A, with 10 μM *cis* Ca^{2+} ($n = 6$ for RyR_N; $n = 5$ for RyR_{MH}) (*A*) or 100 μM *cis* Ca^{2+} ($n = 6$ for RyR_N; $n = 8$ for RyR_{MH}) (*B*). The [Ca^{2+}] was the same in the peptide-containing solution and the perfusion solution. Filled bins, I′p/I′c (see legends to Figs. 5 and 6, for definition) during exposure to 30 μM peptide A. Cross-hatched bins, I′p/I′c for 60 s of maximum activity, 6 to 8 min after washout of peptide A. The asterisks indicate that the difference between I′p/I′c before and after peptide removal is significant according to the Student's *t*-test. The hatch marks (#) indicate the difference is significant according to the nonparametric sign test. Results are shown for −40 mV and +40 mV as indicated.

I′p/I′c after washout at +40 mV. This may have been due to slower removal of the stronger inhibition of RyR_{MH}

Washout activation provides minimum values for the effectiveness of the peptide in activating RyRs, since maximum I′p/I′c occurred when some inhibition remained and activation was declining. Slower washout of inhibition in RyR_{MH} would further reduce the observable activation for these channels. The greatest average activation was a sevenfold increase in I′p/I′c in RyR_N and an 11-fold increase in RyR_{MH} (with 10 μM *cis* Ca^{2+}). Highest individual values were a 12-fold increase in one RyR_N channel and a 15-fold increase in one RyR_{MH}.

Control experiments

Three types of control experiment for the effects of peptide A and its removal on RyR activity are shown in Fig. 10. In the first type of experiment (Fig. 10, *A* and *B*), bilayers were exposed to one concentration of peptide (30 μM) for 20 min. There was a slow increase in activity during the 20 min of exposure to the peptide in RyR_N and RyR_{MH}, with a greater increase in RyR_{MH}. The small increase in activity during exposure to peptide was followed by a massive increase upon washout. Similar results were obtained in 5 bilayers containing RyR_{MH} and 3 bilayers containing RyR_N channels. Fig. 10, *A* and *B*, show examples of washout effects with 300 nM *cis* Ca^{2+} (not shown in Fig. 9 above) and also show that the washout-induced increase in activity after 20 min exposure to 30 μM peptide was similar to that after 2 min exposure to 30 μM peptide, with a total exposure to increasing peptide concentration of 12 min (Fig. 4 above). Thus, the increase in activity after 12 min was a specific effect of washout and not a function of time after exposure to peptide.

In the second type of experiment the volumes of water normally added with peptide were added at the usual intervals, but in the absence of peptide, and then the *cis* chamber perfused (Fig. 10, *C* and *D*, circles). Finally, in the third type of experiment, the *cis* solution was stirred at 2min intervals, with no additions, and then perfused after 12 min (Fig. 10 *D*, triangles). There was no significant increase in RyR_N activity with water or with stirring alone. Neither did activity increase in RyR_N after perfusion. There was a consistent approximately twofold increase in I′ in RyR_{MH} after the second perfusion of the *cis* solution in RyR_{MH}, after either water addition or stirring alone (all experiments were preceded by a perfusion step to replace the incorporation solution with the recording solution; see Methods). The increase after the second perfusion was small compared with the increase in activity after washout of peptide. Similar results were obtained for the water control in 4 bilayers containing RyR_N and 10 bilayers containing RyR_{MH}, and for the stirring controls in 3 bilayers containing RyR_{MH}. Fig. 10, *C* and *D*, shows that the increase in activity during exposure to the peptide and upon its washout are specific effects of peptide A on channel activity, since they do not occur in the absence of peptide.

Fig. 10

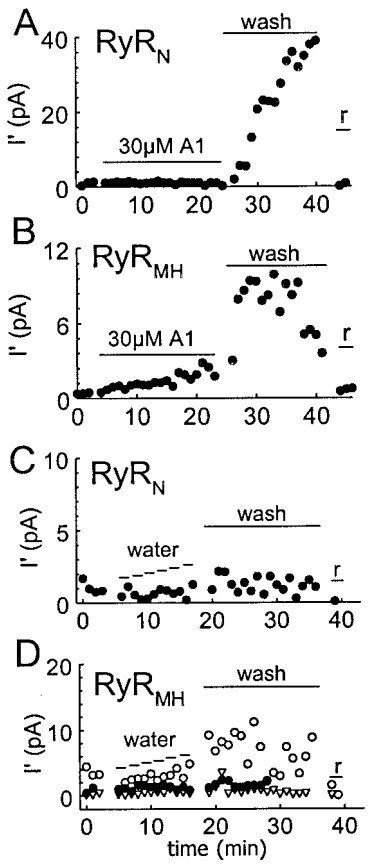

FIGURE 10 A large increase in channel activity upon washout of peptide A occurs after 20 min exposure to 30 μM peptide and is not seen unless channels have been exposed to peptide. Analysis of continuous channel activity in 30-s segments at −40 mV (each separated by a 30-s recording at +40 mV), recorded with 300 nM *cis* Ca^{2+}. The data in *A* and *B* were from a single RyR_N (*A*) and a single RyR_{MH} channel (*B*), under control conditions (first 3 points), during exposure to *cis* peptide for 20 min (30 μM, A1), and after perfusion of the *cis* chamber (wash) and then exposure to ruthenium red (r). The data in *C* were obtained from a bilayer containing two RyR_N channels, under control conditions (first 4 points) during exposure to increasing volumes of water (0.5, 4.5, 4.5, 4.5, 4.5, and 20 μl, equivalent to that added with stock solutions to give 0.6 nM, 6 nM, 60 nM, 0.6 μM, 6 μM, and 30 μM peptide, respectively), and then after perfusion of the *cis* chamber. The data in *D* were from three different bilayers containing RyR_{MH} channels. The open circles show data from one bilayer containing three channels and the filled circles show data from a second bilayer containing one channel. The first two or three data points were obtained under control conditions; data were then obtained with water additions (as above) and after perfusion of the cis chamber, and finally after addition of ruthenium red (r). In the third experiment (*D*, △), data are shown from one channel under control conditions (first 3 points), and then during a 12-min period during which the *cis* solution was stirred every 2 min, but no additions were made to the solution. Perfusion was performed in the usual way after 12 min, and ruthenium red was added at the end of the experiment.

Long-lasting substate openings induced by peptide A

Channel opening to lower conductance levels as a result of the inhibitory action of peptide A was seen in all channels. Very long lasting substate openings (Tripathy et al., 1998; Gurrola et al., 1999) were seen only in a subpopulation of RyR_N and RyR_{MH} and usually in channels that showed strong substate activity under control conditions (Fig. 11, *A* and *B*). There was no consistent difference between RyR_N and RyR_{MH} in substate levels or in the prolongation of substates in the presence of the peptide. Thus an example from one type of channel only is shown in Fig. 11. The predominant substate level in the RyR_{MH} channel in Fig. 11 was at ~33% of the maximum conductance under control conditions and the prolonged substate opening in the presence of 0.6 μM peptide A was to the same level. This level (arrow) is clearly seen in the all points histograms in Fig. 11, *C* and *D*. Twelve of 27 RyR_N and 15 of 23 RyR_{MH} showed substate activity that was prolonged in the presence of the peptide.

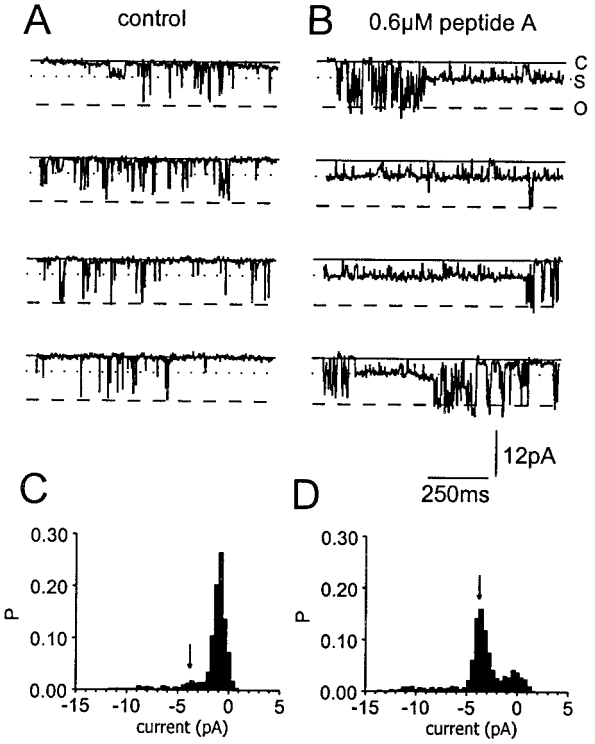

FIGURE 11 Openings to submaximal conductance levels are prolonged by peptide A. The recordings in (*A*) and (*B*) show 4 s of continuous recording from an RyR_{MH} channel at −40 mV with 10 μM *cis* Ca^{2+}, before (*A*) and after (*B*) addition of 0.6 μM peptide A to the *cis* chamber. The solid line (C) shows the zero current, closed level; the dotted line (S) shows the dominant submaximal conductance level which is the same in control activity and after peptide addition. The broken line (O) shows the maximum open single channel conductance. (*C*) and (*D*) are all-points histograms showing the probability (*P*) of current levels (I(pA)) for the data in (*A*) and (*B*), respectively. The closed level at 0 pA is apparent in both histograms. The submaximal level at ~3.8 pA is indicated by the arrow and is clearly enhanced after peptide A addition (*D*).

Effects of control peptides on single channel activity

The specificity of the native sequence of peptide A was examined by adding peptide NB or peptide AS to the *cis* solution while recording activity from RyR_N and RyR_{MH} in the presence of 10 μM *cis* Ca^{2+}, where peptide A induced the strongest activation. Peptide NB had no effect on RyR_N or RyR_{MH} at either −40 mV or +40 mV (Fig. 12, *A* and *B*). Peptide AS did not alter RyR_N activity at +40 mV or −40 mV or RyR_{MH} at +40 mV. Mean current increased by

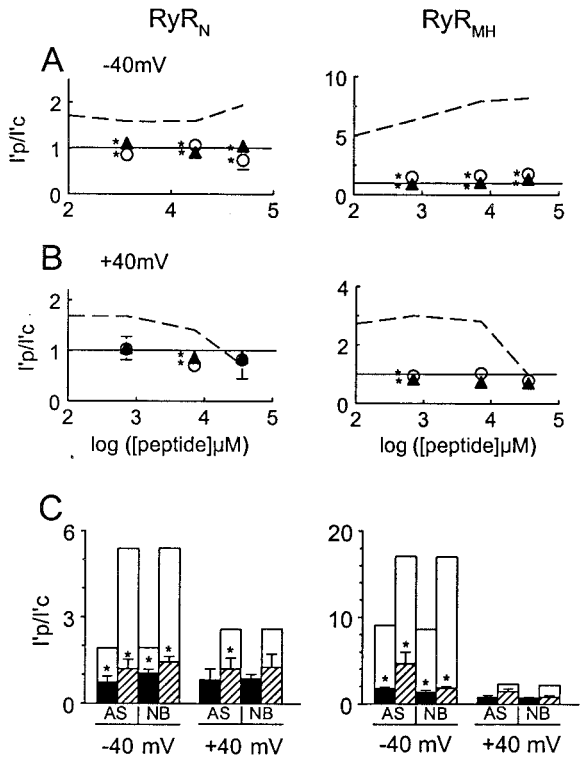

FIGURE 12 Control peptides NB and AS do not reproduce the effects of peptide A on RyR_N or RyR_{MH} with 10 μM *cis* $[Ca^{2+}]$. (*A* and *B*) Relative mean current (I′p/I′c) for RyR_N (left) and RyR_{MH} (right) at −40 mV (*A*) and +40 mV (*B*). Open circles show average data for peptide AS (n = 3, RyR_N; n = 4, RyR_{MH}) and closed triangles show average data for peptide NB (n = 4, RyR_N; n = 5, RyR_{MH}). The broken lines, included for comparison, connect data for peptide A (from Figs. 5 and 6). Asterisks indicate significant differences between either peptide NB or peptide AS and peptide A at each concentration. (*C*) Effects on relative mean current through RyR_N (left) or RyR_{MH} (right) of removing 30 μM of peptides AS or NB from the *cis* chamber. Average I′p/I′c is shown in the presence of 30 μM peptide AS or NB (filled bins) and 3 to 5 min after removal of AS or NB (cross-hatched bins). For comparison, the open bins show average I′p/I′c before and after removal of 30 μM peptide A (data from Fig. 7). Asterisks indicate significant differences between control peptide (NB or AS, data bins) and peptide A (open bins), under each condition.

1.8-fold with 6 μM AS at −40 mV, but this was significantly less than the 7.5-fold increase seen with peptide A.

No significant washout activation was seen with NB or with AS in RyR_N or RyR_{MH} at either −40 or +40 mV (Fig. 12 *C*). An increase in activity was, however, seen in 3 out of 3 RyR_{MH} channels at −40 mV after removal of AS, but the average relative mean current of 4.6 ± 1.4 was significantly less than the average of 11.2 ± 1.2 seen after washout of peptide A. When comparing AS or NB data with peptide A data, the relative mean current at −40 mV was significantly less both before and after washout of AS or NB than before and after washout of peptide A.

Thus, the degree of activation of RyR_N and RyR_{MH} by peptide A was a specific effect of the peptide and depended on the sequence of amino acids in the peptide. The small activation of single channels by the scrambled sequence AS at high peptide concentrations is consistent with the small increase in Ca^{2+} release from SR vesicles evoked by the peptide.

The experiments in Fig. 12 do not provide information on the ability of the control peptides to inhibit RyR activity, since inhibition is minimal when *cis* [Ca^{2+}] is 10 μM (Fig. 8 and Dulhunty et al., 1999), but is significant with 100 μM *cis* Ca^{2+}. Therefore, inhibition by the control peptides was examined in a separate series of experiments with 100 μM *cis* Ca^{2+} and also 2 mM *cis* Na_2ATP (which suppresses activation, but not inhibition, by peptide A; see Results above). Under these conditions, peptide NB failed to inhibit either RyR_N or RyR_{MH} at either −40 mV or +40 mV (Table 2). On the other hand, 6 μM peptide AS inhibited RyR_{MH} at −40 mV, whereas 0.6 μM and 6 μM AS inhibited RyR_{MH} at +40 mV. Peptide AS did not alter activity in RyR_N. These results are consistent with a previous report that AS can inhibit RyR activity (Dulhunty et al., 1999) and confirm the observation that RyR_{MH} is more susceptible than RyR_N to inhibition by positively charged peptides.

TABLE 2 Peptide AS blocks RyR_{MH} activity.

Peptide concentration	*n*	0.6 μM	3 μM	6 μM
			I′p/I′c	
−40 mV				
NB				
RyR_N	6	0.71 ± 0.16	0.90 ± 0.15	0.83 ± 0.16
RyR_{MH}	8	0.89 ± 0.16	0.76 ± 0.25	0.78 ± 0.28
AS				
RyR_N	6	1.07 ± 0.17	—	1.06 ± 0.13
RyR_{MH}	6	0.92 ± 0.17	—	**0.63 ± 0.12**
+40 mV				
NB				
RyR_N	6	1.58 ± 0.44	1.61 ± 0.51	1.36 ± 0.42
RyR_{MH}	8	0.86 ± 0.45	0.74 ± 0.25	0.96 ± 0.29
AS				
RyR_N	6	0.82 ± 0.18	—	0.56 ± 0.14
RyR_{MH}	6	**0.45 ± 0.09**	—	**0.35 ± 0.12**

Effects of peptides **NB** and **AS** on normalized average mean current (I′p/I′c) for RyR_N and RyR_{MH} with 100 μM *cis* Ca^{2+} and 2 mM Na_2ATP, at −40 mV and +40 mV. Data are given as mean ± SEM. **Bold print** indicates a significant (by Student's *t*-test) decrease in mean current in the presence of the peptide.

DISCUSSION

We show here that Ca^{2+} release from the SR of MH-susceptible pig skeletal muscle is more strongly activated by the peptide A segment of the skeletal DHPR II-III loop than Ca^{2+} release from SR of normal pig muscle. In addition, the peptide A-induced increase in RyR channel activity in lipid bilayers was greater in RyR_{MH}. These results suggest that enhanced tension production (Gallant et al., 1980; Ohta et al., 1989) in MH could, in part, be due to stronger activation of RyRs by the A region of the DHPR II-III loop. This would be consistent with observations that MH muscles are more sensitive than normal to some, but not all, RyR agonists, e.g., caffeine, halothane, and ryanodine (Mickelson and Louis, 1996), but not sulfydryl oxidation (Haarmann et al., 1999).

Activation by peptide A

MH mutations might influence relatively distant sites within the RyR. Identified RyR-linked MH mutations occur in two widely separated clusters: between N-terminal residues 35 and 615 (MH_1 domain) and between residues 2163–2458 (MH_2 domain; Tong et al., 1997). The only direct comparison of mutations from these two domains found that the physiological abnormalities were nearly identical (Richter et al., 1997). It is possible that the MH domains of the RyR are structurally important and/or have allosteric effects over widespread areas of the RyR. The $Arg^{615}Cys$ substitution could alter the conformation of the MH_1 domain and its interaction with other regions of the RyR or allosterically alter the II-III loop binding site or the structure of regions critical for transmission of information from the DHPR binding region to the RyR ion channel pore.

It is not possible, from the present experiments, to distinguish among several likely mechanisms for stronger activation of RyRs by peptide A. The MH mutation may alter the peptide binding site on the RyR so that the peptide binds more effectively and causes greater activation. A second possibility is that the MH mutation facilitates transmission of a signal from the remote cytoplasmic DHPR-binding domain, presumably adjacent to the T-tubule membrane, to the channel gating mechanism. Alternatively, the response of the RyR gating mechanism to a signal from the binding domain might be facilitated. In the last case, any activating signal should induce a stronger response in RyR_{MH} than in RyR_N. This is not the case, because the increase in activity upon sulfhydryl oxidation is not greater in RyR_{MH} (Haarmann et al., 1999).

We have suggested that the A region of the DHPR is bound to the RyR in resting muscle (Dulhunty et al., 1999). Increased resting activation of RyR_{MH} by the A region in vivo could contribute to enhanced Ca^{2+}-activated Ca^{2+} release (Kim et al., 1984; Ohta et al., 1989; Mickelson et al., 1988) and increased force (Gallant et al., 1980). If mechanisms that lower myoplasmic [Ca^{2+}] are unable to cope with the high Ca^{2+} leak, resting cytoplasmic [Ca^{2+}] would also be higher than normal (Lopez et al., 1986).

The scrambled peptide AS released Ca^{2+} from SR_{MH}, and from rabbit skeletal SR, at a lower rate than the native peptide A (Dulhunty et al., 1999) and enhanced RyR_{MH} activity. Since peptide AS contains the same number of positively charged residues as peptide A, it is likely that it interacts weakly with the A-binding region on the RyR, but cannot interact strongly because it lacks the appropriate structure (Casarotto et al., 2000).

Inhibition

Inhibition by high concentrations of the peptide A at +40 mV was enhanced by the MH mutation. The voltage and current direction dependence of inhibition suggest that the peptide blocks the channel pore (Dulhunty et al., 1999) as a result of strong interactions between its numerous positively charged residues and negative sites within the pore (Mead et al., 1998). In contrast, activation is likely to depend on peptide binding to a II-III loop binding-site on the RyR. The enhanced inhibition of RyR_{MH} could be due to a greater negative charge density in the channel vestibule as result of the $Arg^{615}Cys$ substitution. Alternatively, the geometry of the vestibule might change to allow the peptide greater accessibility. In either case, the results show that the MH mutation changes more than one property of the RyR and underlines the importance of the MH domains in influencing the structure of the entire RyR. The MH mutation in the N-terminal part of the RyR alters the properties of C-terminal residues, which form the channel pore (Bhat et al., 1997).

Inhibition by peptide A was not apparent in Ca^{2+} release from SR_N and SR_{MH} and is not apparent in Ca^{2+} release from rabbit skeletal SR (Dulhunty et al., 1999). Inhibition is minimal in these experiments where ion flow is from the SR lumen into the cytoplasm. Inhibition is strongest when ions flow from the cytoplasm to the lumen (i.e., +40 mV). It is unlikely that inhibition occurs in vivo where the II-III loop is tethered to the DHPR in the T-tubule membrane well away from the RyR pore.

Multiple effects of the MH mutation

In addition to effects of the MH mutation on activation and inhibition by peptide A, the $Arg^{615}Cys$ substitution is associated with a reduced affinity of RyR_{MH} for Ca^{2+} (Fill et al., 1991; Shomer et al., 1993; Richter et al., 1997) or Mg^{2+} (Laver et al., 1997) at a low affinity inhibitory site. We did not use [Ca^{2+}] in the inhibitory range (>100 μM), so did not observe this difference between RyR_{MH} and RyR_N. Mg^{2+} inhibition is thought to play a critical role in EC coupling in that the RyR is chronically inhibited at myoplasmic [Mg^{2+}]. Ca^{2+} release during EC coupling proceeds because the EC coupling signal from the DHPR reduces the affinity of the RyR for Mg^{2+} (Lamb and Stephenson, 1991). The lower than normal affinity of RyR_{MH} for Mg^{2+} means that RyR activity is higher than normal and may be enhanced more than normal during EC coupling (Laver et al., 1997). The Ca^{2+}/Mg^{2+} inhibition site has been located on the C-terminal portion of the RyR (3692 to 4969, Lynch et al., 1999), and changes to this site might be related to changes in the channel region that lead to enhanced inhibition by peptide A. Involvement of the C-terminal Mg^{2+}-inhibition region further emphasizes the wide-spread influence of the MH domain on RyR structure and function.

As mentioned previously, it is not clear whether the MH mutation increases the ability of all activating agents to enhance channel activity by altering a common site in the activation process or whether the mutation causes multiple changes in ligand binding sites or links between the binding sites and the channel pore. Both activation by relief of Mg^{2+} inhibition (with reduced [Mg^{2+}]) and by caffeine are enhanced in MH, suggesting that both physiological and nonphysiological activators may share a common activation mechanism. On the other hand, physiological activation by sulfhydryl oxidation is not enhanced in MH (Haarmann et al., 1999), so that the common mechanism is not shared by all activating influences. Thus, the question remains open whether peptide A is a physiological or a nonphysiological activator of the RyR channel, since the A region is not essential for skeletal EC coupling (Nakai et al., 1998, 2000). The peptide, however, has several merits as a probe for studying normal and disordered RyR activity, including its high affinity and specific binding to the calcium release channel.

Peptide A-evoked Ca^{2+} release from normal pig SR

The low Ca^{2+} release from SR_N induced by peptide A was unexpected, since EC coupling and contraction in pig muscle proceed as effectively as in rabbit muscle (Gallant et al., 1980). In contrast to Ca^{2+} release, activation of single pig RyR_N channels by peptide A was similar to activation of rabbit RyRs (Dulhunty et al., 1999). Ca^{2+} release from the SR was, of necessity, measured in the presence of ATP, which prevented peptide A activation of single pig RyR channels (Results). Thus ATP may have suppressed Ca^{2+} release from pig SR. We are further investigating this effect of ATP on peptide A activation of pig RyRs.

There are several possible reasons for the difference between peptide A-induced activation of normal pig and rabbit RyRs. Rabbit and pig RyRs differ by one amino acid in the RyR sequence required for DHPR II-III loop binding with $Thr^{1082}Ala$ substitution in the pig (Fujii et al., 1991; Takeshima et al., 1989). First, this difference may destabilize peptide A binding and reduce in vitro peptide A activation of normal pig RyRs (in vivo, the RyR-DHPR loop interaction could be stabilized by the spatial constraints imposed by insertion of the two large proteins in their respective membranes). Second, the sequence differences between normal pig and rabbit RyRs may mean that additional cytosolic factors are necessary for effective peptide A, or A region of the II-III loop, binding to the RyR in normal pig muscle. Finally, there maybe be changes in the porcine II-III loop sequence that accommodate and stabilize binding to the porcine RyR_N. A number of species-specific sequence differences occur in the DHPR II-III loop, although the pig sequence is not yet reported (Tanabe et al., 1987; Hogan et al., 1994; Chaudhari, 1992). In any case, the lack of peptide A sensitivity of normal pig RyRs in vitro in the presence of ATP is partially reversed by the MH mutation.

In conclusion, we find that RyR channels from MH-susceptible pig muscle are more easily activated by peptide A than RyR channels from normal pigs, in the absence of Mg^{2+} or inhibiting concentrations of cytoplasmic Ca^{2+}. The channels from MH-susceptible muscle are also inhibited more by high concentrations of the positively charged peptide. The results suggest that activation by the DHPR II-III loop might be enhanced during EC coupling and contribute to an increase in Ca^{2+} release from the SR of MH-susceptible muscle. In addition, the results show that the MH point mutation alters the response of the RyR to more than one ligand, and thus has multiple actions on the RyR.

We thank Joan Stivala for general assistance and Dr. J. R. Mickelson for help with sequence information. Dr. Gallant was on sabbatical leave from the Department of Veterinary Pathobiology, University of Minnesota (St. Paul, MN) and received funding from the National Science Foundation (INT-9724904) and the National Institutes of Health (AR08477).

REFERENCES

Bhat, M. B., J. Zhao, H. Takeshima, and J. Ma. 1997. Functional calcium release channel formed by the carboxyl-terminal portion of ryanodine receptor. *Biophys. J.* 73:1329–1336.

Casarotto, M. G., F. Gibson, S. M. Pace, S. M. Curtis, M. Mulcair, and A. F. Dulhunty. 2000. A structural requirement for activation of skeletal RyRs by a 20 amino acid region of the II-III loop of the skeletal DHPR. *J. Biol. Chem.* 275:11631–11637.

Chaudhari, N. 1992. A single nucleotide deletion in the skeletal muscle specific transcript of muscular dysgenisis (mdg) mice. *J. Biol. Chem.* 267:25636–25639.

Dulhunty, A. F., D. R. Laver, E. M. Gallant, M. G. Casarotto, S. M. Pace, and S. Curtis. 1999. Activation and inhibition of skeletal RyR channels by a part of the skeletal DHPR II-III loop: effects of DHPR Ser^{687} and FKBP12. *Biophys. J.* 77:189–203.

El-Hayek, R., B. Antoniu, J. Wang, S. L. Hamilton, and N. Ikemoto. 1995. Identification of calcium release-triggering and blocking regions of the II-III loop of the skeletal muscle dihydropyridine receptor. *J. Biol. Chem.* 270:22116–22118.

El-Hayek, R., and N. Ikemoto. 1998. Identification of the minimum essential region in the II-III loop of the dihydropyridine receptor a1 subunit required for activation of skeletal muscle-type excitation-contraction coupling. *Biochemistry.* 37:7015–7020.

Fill, M., E. Stefani, and T. E. Nelson. 1991. Abnormal human sarcoplasmic reticulum Ca^{++} release channels in malignant hyperthermic skeletal muscle. *Biophys. J.* 59:1085–1090.

Fujii, J., K. Otsu, F. Zorzato, S. De Leon, V. K. Khanna, J. E. Weiler, P. J. O'Brien, and D. H. Maclennan. 1991. Identification of a mutation in porcine ryanodine receptor associated with malignant hyperthermia. *Science.* 253:448–451.

Gallant, E. M., R. E. Godt, and G. A. Gronert. 1980. Mechanical properties of normal and malignant hyperthermia susceptible porcine muscle: effects of halothane and other drugs. *J. Pharmacol. Exp. Ther.* 213:91–96.

Gurrola, G. B., C. Arevalo, R. Sreekumar, A. J. Lokuta, J. W. Walker, and H. H. Valdivia. 1999. Activation of ryanodine receptors by imperatoxin A and a peptide segment of the II-III loop of the dihydropyridine receptor. *J. Biol. Chem.* 274:7879–7886.

Haarmann, C. S., R. A. H. Fink, and A. F. Dulhunty. 1999. Oxidation and reduction of pig skeletal ryanodine receptors. *Biophys. J.* 77:3010–3022.

Hogan, K., P. A. Powers, and R. G. Gregg. 1994. Cloning of the human skeletal muscle α_1 subunit of the dihydropyridine-sensitive L-type calcium channel (CACNL1A3). *Genomics.* 24:608–609.

Jurkat-Rott, K., T. McCarthy, and F. Lehmann-Horn. 2000. Genetics and pathogenesis of malignant hyperthermia. *Muscle Nerve.* 23:4–17.

Kim, D. H., F. A. Sreter, S. T. Ohnishi, J. F. Ryan, J. Roberts, P. D. Allen, L. G. Meszaros, B. Antoniu, and N. Ikemoto. 1984. Kinetic studies of Ca^{2+} release from sarcoplasmic reticulum of normal and malignant hyperthermia susceptible pig muscles. *Biochim. Biophys. Acta.* 775: 320–327.

Lamb, G. D., and D. G. Stephenson. 1991. Effect of Mg^{++} on the control of Ca^{++} release in skeletal muscle fibres of the toad. *J. Physiol.* 434:507–528.

Laver, D. R., V. J. Owen, P. R. Junankar, N. L. Taske, A. F. Dulhunty, and D. G. Lamb. 1997. Reduced inhibitory effect of Mg^{2+} on ryanodine receptor Ca^{2+} release channels in Malignant Hyperthermia. *Biophys. J.* 73:1913–1924.

Leong, P., and D. H. Maclennan. 1998. A 37-amino acid sequence in the skeletal muscle ryanodine receptor interacts with the cytoplasmic loop between domains II and III in the skeletal muscle dihydropyridine receptor. *J. Biol. Chem.* 273:7791–7794.

Loke, J., and D. H. Maclennan. 1998. Malignant hyperthermia and central core disease: disorders of Ca^{2+} release channels. *Am. J. Med.* 104: 470–486.

Lopez, J. R., L. A. Alamo, D. E. Jones, L. Papp, P. D. Allen, J. Gergely, and F. A. Sreter. 1986. Ca^{++} in muscles of malignant hyperthermia susceptible pigs determined in vivo with Ca^{++} selective microelectrodes. *Muscle Nerve.* 9:85–86.

Lu, X., L. Xu, and G. Meissner. 1994. Activation of the skeletal muscle calcium release channel by a cytoplasmic loop of the dihydropyridine receptor. *J. Biol. Chem.* 269:6511–6516.

Lu, X., L. Xu, and G. Meissner. 1995. Phosphorylation of dihydropyridine receptor II-III loop peptide regulates skeletal muscle calcium release channel function. *J. Biol. Chem.* 270:18459–18464.

Lynch, P. J., J. Tong, M. Lehane, A. Mallet, L. Giblin, J. J. Heffron, P. Vaughan, G. Zafra, D. H. Maclennan, and T. V. McCarthy. 1999. A mutation in the transmembrane/luminal domain of the ryanodine receptor is associated with abnormal Ca^{2+} release channel function and severe central core disease. *Proc. Natl. Acad. Sci. USA.* 96:4164–4169.

Ma, J. 1995. Desensitization of the skeletal muscle ryanodine receptor: evidence for heterogeneity of calcium release channels. *Biophys. J.* 68:893–899.

Mead, F. C., D. Sullivan, and A. J. Williams. 1998. Evidence for a negative charge in the conduction pathway of the cardiac ryanodine receptor channel provided by the interaction of K^+ channel N-type inactivation peptides. *J. Membr. Biol.* 163:225–234.

Meissner, G. 1984. Adenine nucleotide stimulation of Ca^{++}-induced Ca^{++} release in sarcoplasmic reticulum. *J. Biol. Chem.* 259:2365–2374.

Mickelson, J. R., E. M. Gallant, L. A. Litterer, K. M. Johnson, W. E. Rempel, and C. F. Louis. 1988. Abnormal sarcoplasmic reticulum ryanodine receptor in malignant hyperthermia. *J. Biol. Chem.* 9310:9315.

Mickelson, J. R., and C. F. Louis. 1996. Malignant Hyperthermia: Excitation-contraction coupling, Ca^{++} release channel, and cell Ca^{++} regulation defects. *Physiol. Rev.* 76:537–592.

Minium, E. W., B. M. King, and G. Bear. 1993. Statistical reasoning in psychology and education. John Wiley & Sons, New York.

Nakai, J., T. Tanabe, T. Konno, B. Adams, and K. G. Beam. 1998. Localization in the II-III loop of the dihydropyridine receptor of a sequence critical for excitation-contraction coupling. *J. Biol. Chem.* 273:24983–24986.

Ohta, T., M. Endo, T. Nakano, Y. Morohoshi, K. Wanikawa, and A. Ohga. 1989. Ca-induced Ca release in malignant hyperthermia-susceptible pig skeletal muscle. *Am. J. Physiol.* 256:C358–C367.

Otsu, K., M. S. Phillips, V. K. Khanna, S. De Leon, and D. H. Maclennan. 1992. Refinement of diagnostic assays for a probable causal mutation for porcine and human malignant hyperthermia. *Genomics.* 13:835–837.

Otsu, K., K. Nishida, Y. Kimura, T. Kuzuya, T. Kamada, and M. Tada. 1994. The point mutation arg^{615}cis in the Ca^{2+} release channel of skeletal sarcoplasmic reticulum is responsible for hypersensitivity to caffeine and halothane in malignant hyperthermia. *J. Biol. Chem.* 269: 9413–9415.

Owen, V. J., N. L. Taske, and G. D. Lamb. 1997. Reduced Mg^{++} inhibition of Ca^{++} release in muscle fibers of pigs susceptible to malignant hyperthermia. *Am. J. Physiol.* 272:C203–C211.

Proenza, C., C. M. Wilkins, and K. G. Beam. 2000. Excitation-contraction coupling is not affected by scrambled sequence in residues 681–690 of the dihydropyridine receptor II-III loop. *J. Biol. Chem.* (in press).

Richter, M., L. Schleithoff, T. Deufel, F. Lehmann-Horn, and A. Herrmann-Frsank. 1997. Functional characterization of a distinct ryanodine receptor mutation in human malignant hyperthermia-susceptible muscle. *J. Biol. Chem.* 272:5256–5260.

Sagara, Y., and G. Inesi. 1991. Inhibition of the sarcoplasmic reticulum Ca^{++} transport ATPase by thapsigargin at subnanomolar concentrations. *J. Biol. Chem.* 266:13503–13506.

Shomer, N. H., C. F. Louis, M. Fill, L. A. Litterer, and J. R. Mickelson. 1993. Reconstitution of abnormalities in the malignant hyperthermia-susceptible pig ryanodine receptor. *Am. J. Physiol.* 264:C125–C135.

Takeshima, H., S. Nishimura, T. Matsumoto, H. Ishida, K. Kangawa, N. Minamino, H. Matsuo, M. Ueda, M. Hanaoka, T. Hirose, and S. Numa. 1989. Primary structure and expression from complementary cDNA of skeletal muscle ryanodine receptor. *Nature.* 339:439–445.

Tanabe, T., H. Takeshima, A. Mikami, V. Flockerzi, H. Takahashi, K. Kangawa, M. Kojima, H. Matsuo, T. Hirose, and S. Numa. 1987. Primary structure of the receptor for calcium channel blockers from skeletal muscle. *Nature.* 328:313–318.

Tanabe, T., K. G. Beam, B. A. Adams, T. Niidome, and S. Numa. 1990. Regions of the skeletal muscle dihydropyridine receptor critical for excitation-contraction coupling. *Nature.* 346:567–568.

Timerman, A. P., E. Ogunbumni, E. Freund, G. Wiederrecht, A. R. Marks, and S. Fleischer. 1993. The calcium release channel of sarcoplasmic reticulum is modulated by FK-506-binding protein. *J. Biol. Chem.* 268:22992–22999.

Tong, J., H. Oyamada, N. Demaurex, S. Grinstein, T. V. McCarthy, and D. H. Maclennan. 1997. Caffeine and halothane sensitivity of intracellular Ca^{2+} release is altered by 15 calcium release channel (ryanodine receptor) mutations associated with malignant hyperthermia and/or central core disease. *J. Biol. Chem.* 272:26332–26339.

Tong, J., T. V. McCarthy, and D. H. Maclennan. 1999. Measurement of resting cytocolic Ca^{2+} concentrations and Ca^{2+} store size in HEK-293 cells transfected with malignant hyperthermia or central core disease mutant Ca^{2+} release channels. *J. Biol. Chem.* 274:693–702.

Tripathy, A., W. Resch, L. Xu, H. H. Valdivia, and G. Meissner. 1998. Imperatoxin A induces subconductance states in Ca^{2+} release channels (ryanodine receptors) of cardiac and skeletal muscle. *J. Gen. Physiol.* 111:679–690.